Microsyst Technol (2014) 20:1653–1659
DOI 10.1007/s00542-014-2206-8

TECHNICAL PAPER

Vibration study and classification of rotor faults in PM synchronous motor

Yinquan Yu · Chao Bi · Quan Jiang · Song Lin · Nay Lin Htun Aung · A. A. Mamun

Received: 8 October 2013 / Accepted: 29 April 2014 / Published online: 20 May 2014

Abstract Thanks for the precision engineering technology, motor, especially Permanent Magnet Synchronous Motor can be made as Micro-motor. However, any imprecise rotor parts of this meticulous motor could lead to undesirable vibration and acoustic noise (Yu et al. in 3D influence of unbalanced magnetic pull induced by misalignment rotor in PMSM, APMRC2012, 2012; Bi et al. in Influence of axial asymmetrical rotor in PMAC motor operation, ICEMS, 2011; Bi et al. in Influence of rotor eccentricity to unbalanced-magnetic-pull in pm synchronous motor, ICEMS06, 2006). This paper presents five types of rotor faults design and vibration study of these five types of faults in motor is conducted. Based on the vibration pattern, fuzzy mathematics is employed to classify these five types of rotor faults.

1 Introduction

Both radial and axial direction Repeatable Run-Out (RRO) and none repeatable Run-Out (NRRO) of spindle motor in HDD is a big concern in high area density requirement. Besides the reasonable spindle motor structure design which studied in (Bi et al. 2006, 1997), the fabrication tolerance of spindle motor parts should be controlled in order to minimum RRO and NRRO. As it is known, the vibration of spindle motor is mainly caused by unreasonable Unbalanced Magnet Pulls (UMPs). Different motor parts faults (tolerance is out of the control) will generate different types of UMPs which lead to different vibration and acoustic noise signals pattern. Though studying different vibration signals and acoustic noise pattern, the types of UMPs or other faults can be detected and classified. Then, the related imprecise parts (out of tolerance controlled) can be known. Although researchers have studied years (Guo et al. 2002; Krysinski and Malburt 2007; "Ninth International Conference on Vibrations in Rotating Machinery volume two, University of Exeter, UK September 8–10 2008"), none of which has classified UMPs and Mechanical Unbalance (MU). In this paper, four types of UMPs related and MU related faulty motors are designed. Fuzzy Mathematics Classification (FMC) is proposed to classify the motor faults. The motor used in the study is a surface mounted PMSM with 12 slots and 5 pole-pairs. This paper can be a guideline of design high performance motor; it also can be the reference of general motor fault diagnosis.

Y. Yu (✉) · C. Bi · Q. Jiang · S. Lin · N. L. H. Aung
Division of Disk Drive System, Data Storage Institute,
A-Star, Singapore 117608, Singapore
e-mail: Yu_YinQuan@dsi.a-star.edu.sg

C. Bi
e-mail: BI_CHAO@dsi.a-star.edu.sg

Q. Jiang
e-mail: Jiang_Quan@dsi.a-star.edu.sg

S. Lin
e-mail: LIN_Song@dsi.a-star.edu.sg

N. L. H. Aung
e-mail: Nay_AUNG@dsi.a-star.edu.sg

A. A. Mamun
Department of Electrical and Computer Engineering,
National University of Singapore,
Singapore 117608, Singapore
e-mail: eleaam@nus.edu.sg

2 Approach

2.1 Experimental specimen design

An oriental motor is modified as M1. One pair of new rear side and load side covers of motor is made to generate various types of eccentricity faults. The modified M1 is used with parameters as given in Table 1 to simulate different eccentricity condition.

Figure 1 shows the structure of modified M1 which is used in the vibration measurement experiment. Two outer rings were purposely press-fitted between the ball bearing and bearing cover at both ends of the shaft. Similarly, two inner rings were press-fitted between the ball bearing and the shaft at both ends. Figure 2 illustrated the rotor structure of M1, and a datum line was marked.

When the inner ring is symmetrical and the outer rings were purposely made unsymmetrical while both were in line with the locating pin, as shown in Fig. 3, static eccentricity (SE) was produced. When the outer ring is symmetrical and the inner one is not, as shown in Fig. 4, dynamic eccentricity (DE) is generated. In this case, the locating marks of the inner rings at both ends had to be in line with the datum line on the shaft (refers to Fig. 2) so that

Table 1 PMSM Specifications

Power	50 W
Rated voltage	24VDC
Pole pairs	P = 5
Phase	3
Speed	Nmax = 3,000 rpm; Nrated = 2,500 rpm
Torque	Mmax = 0.24 N M; Mrated = 0.2 N M
Current	Imax = 5.4 A; Irated = 3.1 A
Rotor inertia	J = 2.34e−5 kg m^2

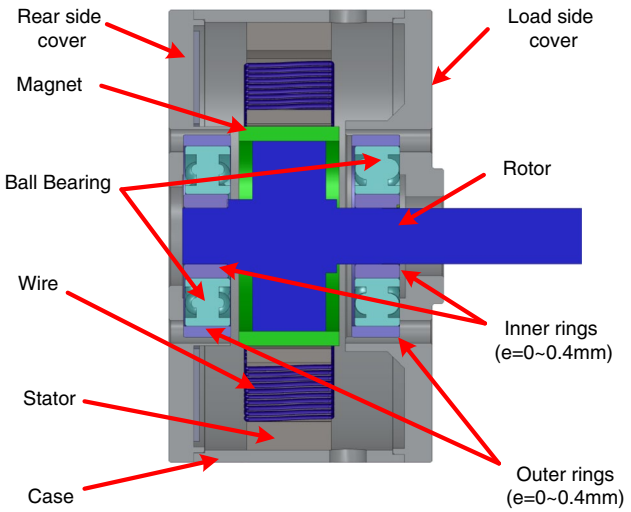

Fig. 1 Modified M1 with difference type of eccentricity

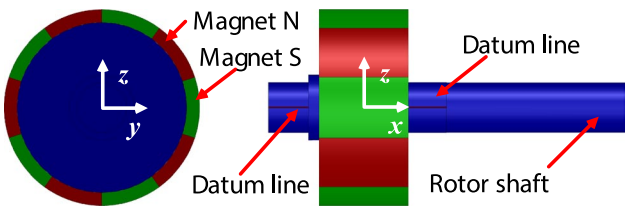

Fig. 2 Rotor structure with *datum line* on rotor shaft

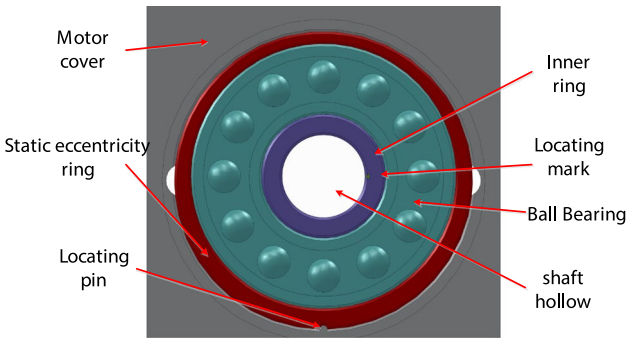

Fig. 3 Structure design to simulate motor SE fault

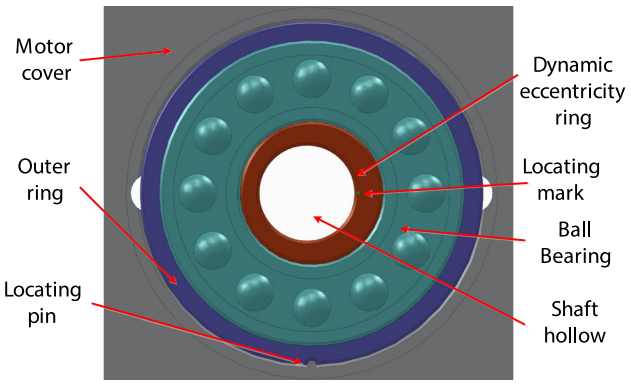

Fig. 4 Structure design to simulate motor DE fault

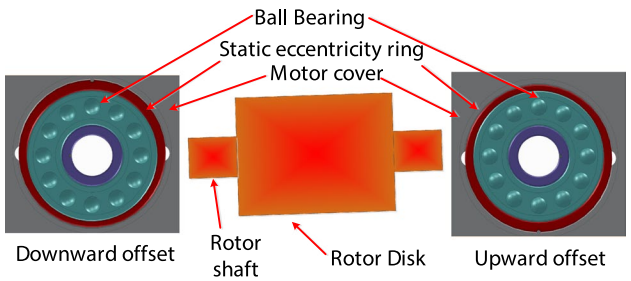

Fig. 5 Structure design to simulate motor IE fault

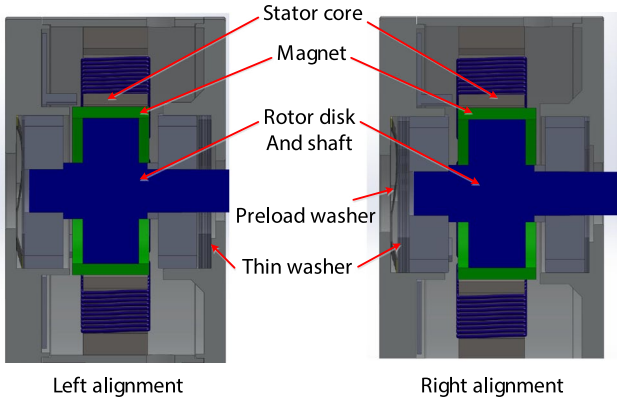

Fig. 6 Motor Structure which has axial eccentricity fault

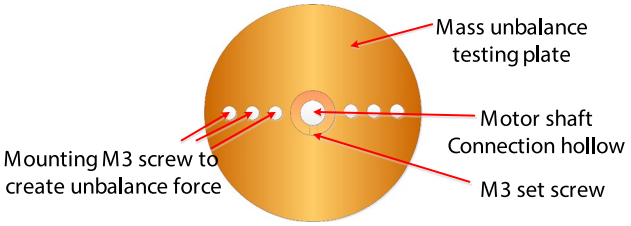

Fig. 7 Mechanical unbalance disk

the dynamic eccentricity at both sides is in phase. A more complicated case, with both the outer rings at both ends made unsymmetrical and opposite in press-fitting direction, an incline eccentricity (IE) was produced, as illustrated in Fig. 5. The grade of eccentricities in SE, DE and IE could be adjusted since the ring thickness range was 0–0.4 mm. Yet another eccentricity case, axial eccentricity (AE), could be created by adding different pieces of thin washers between two bearings and bearing covers in axial direction, as shown in Fig. 6.

Mechanical unbalance in this study was simulated by attaching an unbalance disk to the motor rotor shaft. There were six Ø3.1 holes symmetrically made at the both side of aluminum disk as shown in Fig. 7, where M3 screw and nut could be mounted to produce unbalanced mass. Based on the weight and position of the mounted screw and nut, different mass unbalance force under different running speed can be calculated.

2.2 Vibration measurement

Figure 8 shows the experimental setup for measuring the vibration induced by MU fault and UMPs related faults such as SE, DE, IE, and AE faults on the anti-vibration table. The modified M1 is mounted on a rigid motor fixture. With the motor was driven at difference

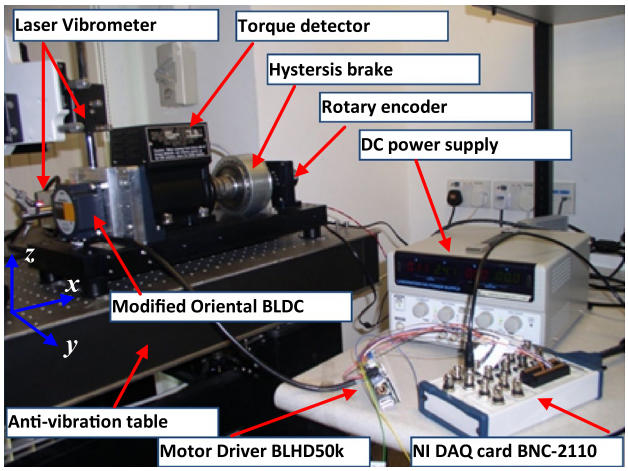

Fig. 8 Rotor eccentricity-induction measurement setup

rotating speeds, a rotary encoder was used to measure motor speed. A hysteresis brake was used to add different loads. Two Laser Doppler Vibrometers (LDVs) were employed to measure the velocity from points on both the motor stationary horizontal and vertical direction, respectively.

The real time vibration data of the motor running at 3,000 rpm in normal state (no eccentricity), SE state, DE state, IE state, and AE state were respectively captured, the FFT resulted calculated, and the frequency components of interest (1×, 10×, 11× and 60×) listed in Table 2 as fault features for eccentricity classification.

When the motor has same pole-pairs and slots configuration as M1, the main faulty frequency of the motor on the SE and IE state is 10× (Yu et al. 2012). On the other hand, the main faulty frequencies of the motor on DE state are 1× and 11× (Bi et al. 2006). Other than on SE, DE, and IE states, the main faulty frequency of the motor on AE state is 60× (Bi et al. 2011). The main faulty frequency of MU is well-known as 1× (Sudhakar and Sekhar 2011; Huang 2007; Concari et al. 2010; Jalan and Mohanty 2009; Kim 2009). So, these four orders frequencies are selected as fault features to classify faulty motor with different types of mechanical and UMPs related eccentricity faults.

In Table 2, vibrating amplitudes at $\boldsymbol{x}$ (axial), $\boldsymbol{y}$ (lateral) and $\boldsymbol{z}$ (vertical) directions with different fault grades were listed versus different frequencies. The contents (e0–e4) in first column of Table 2 stand for 0–0.4 mm eccentricity faults, respectively. The columns with bold font are the dominant fault features for different eccentricities, since the variations of values in bold font columns are much larger than those in other columns when the fault grade is changed. It was also noted that the frequencies of faulty features are different when the motor

Table 2 Extracted signals of normal and faulty motor

Fault grades	x (m/s)				y (m/s)				z (m/s)			
	50 Hz	500 Hz	550 Hz	3,000 Hz	50 Hz	500 Hz	550 Hz	3,000 Hz	50 Hz	500 Hz	550 Hz	3,000 Hz
(a) Normal motor												
No fault	0.016604	0.205243	0.024461	0.018985	0.028978	0.161224	0.022174	0.018481	0.034774	0.193543	0.026484	0.022185
(b) MU result with different fault grades												
e0	0.016600	0.205200	0.024460	0.018980	**0.028980**	0.161200	0.022170	0.018480	**0.034770**	0.193500	0.026480	0.022180
el	0.016623	0.205234	0.024498	0.019010	**0.029965**	0.161233	0.022189	0.018512	**0.037000**	0.193519	0.026513	0.022219
e2	0.016638	0.205239	0.024483	0.019014	**0.030330**	0.161222	0.022206	0.018507	**0.038330**	0.193536	0.026484	0.022208
e3	0.016623	0.205235	0.024502	0.019045	**0.031500**	0.161219	0.022197	0.018522	**0.039690**	0.193526	0.026515	0.022212
e4	0.016625	0.205226	0.024498	0.019009	**0.033820**	0.161212	0.022218	0.018499	**0.044620**	0.193534	0.026529	0.022212
(c) SE result with different fault grades												
e0	0.016600	0.205200	0.024460	0.018980	0.028980	**0.161200**	0.022170	0.018480	0.034770	**0.193500**	0.026480	0.022180
el	0.016622	0.205255	0.024504	0.019021	0.028991	**0.161657**	0.022212	0.018514	0.034798	**0.194342**	0.026505	0.022202
e2	0.016626	0.205217	0.024473	0.019011	0.029006	**0.162148**	0.022205	0.018507	0.034803	**0.195244**	0.026529	0.022200
e3	0.016628	0.205231	0.024509	0.019033	0.029002	**0.162625**	0.022210	0.018501	0.034810	**0.196455**	0.026508	0.022214
e4	0.016625	0.205216	0.024479	0.019038	0.029002	**0.163222**	0.022209	0.018516	0.034804	**0.198356**	0.026508	0.022226
(d) DE result with different fault grades												
e0	0.016600	0.205200	0.024460	0.018980	**0.028980**	0.161200	**0.022170**	0.018480	**0.034770**	0.193500	**0.026480**	0.022180
el	0.016639	0.205237	0.024496	0.019026	**0.030511**	0.161242	**0.023701**	0.018507	**0.034790**	0.038013	**0.029723**	0.022201
e2	0.016643	0.205217	0.024480	0.018995	**0.031675**	0.161222	**0.024865**	0.018528	**0.034797**	0.041140	**0.032850**	0.022212
e3	0.016605	0.205220	0.024474	0.018997	**0.033013**	0.161217	**0.026203**	0.018519	**0.034814**	0.044440	**0.036150**	0.022226
e4	0.016628	0.205238	0.024498	0.018995	**0.034479**	0.161229	**0.027669**	0.018509	**0.034815**	0.048080	**0.039790**	0.022211
(e) IE result with different fault grades												
e0	0.016600	0.205200	0.024460	0.018980	0.028980	0.161200	0.022170	0.018480	0.034770	0.193500	0.026480	0.022180
el	0.016635	0.205948	0.024486	0.019016	0.029009	0.161429	0.022194	0.018504	0.034789	0.193866	0.026503	0.022203
e2	0.016627	0.209270	0.024492	0.019013	0.029003	0.161625	0.022205	0.018510	0.034810	0.194233	0.026507	0.022201
e3	0.016634	0.214970	0.024482	0.019014	0.029013	0.161861	0.022200	0.018537	0.034803	0.195034	0.026495	0.022206
e4	0.016629	0.227510	0.024477	0.019001	0.029034	0.162219	0.022200	0.018499	0.034807	0.196220	0.026501	0.022201
(f) AE result with different fault grades												
e0	0.016600	0.205200	0.024460	**0.018980**	0.028980	0.161200	0.022170	0.018480	0.034770	0.193500	0.026480	0.022180
el	0.016622	0.205255	0.024504	**0.028925**	0.028991	0.161231	0.022212	0.018514	0.034798	0.193533	0.026505	0.022202
e2	0.016626	0.205217	0.024473	**0.039770**	0.029006	0.161251	0.022205	0.018507	0.034803	0.193531	0.026529	0.022200
e3	0.016628	0.205231	0.024509	**0.058460**	0.029002	0.161223	0.022210	0.018501	0.034810	0.193522	0.026508	0.022214
e4	0.016625	0.205216	0.024479	**0.097040**	0.029002	0.161227	0.022209	0.018516	0.034804	0.193538	0.026508	0.022226

Bold values indicate the dominant frequency of vibration induced by each type of UMPs faults

has different types of eccentricities. Such obviously distributed fault feature patterns provide strong support for the application of fuzzy mathematics for fault classification.

2.3 Faults classification by fuzzy mathematics

2.3.1 Introduction of fuzzy mathematics

Fuzzy mathematics is a multi-targets decision making mathematics model. Fuzzy mathematics for faults diagnosis and classification consists of two main steps, first of which is to build fuzzy transformation matrix [Eq. (3)] between feature vector [Eq. (1)] and fault vector [Eq. (2)].

$$V = [v_1,\ v_1, \ldots, v_m] \tag{1}$$

$$U = [u_1,\ u_1, \ldots, u_m] \tag{2}$$

$$R = \begin{bmatrix} r_{11} & r_{12} & \cdots & r_{13} \\ r_{21} & r_{22} & \cdots & r_{23} \\ \cdots & \cdots & \cdots & \cdots \\ r_{n1} & r_{n2} & \cdots & r_{nm} \end{bmatrix} \tag{3}$$

Raw data of different fault features may have different measuring units or different value levels. In order to

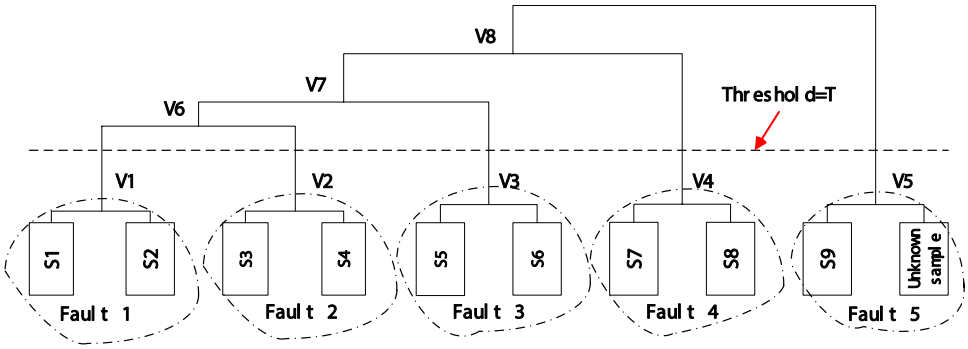

Fig. 9 The fault classification structure

Fig. 10 The standardized fuzzy matrix

	No fault	Mechanical unbalance	Static eccentricity	Dynamic eccentricity	Incline eccentricity	Axial eccentricity
1X	-1.7264	-0.3069	0.1619	1.3108	0.3895	0.1711
10X	-0.4712	-0.3789	-0.4258	-0.4136	2.0395	-0.3499
11X	-1.7681	0.9811	0.9408	-0.1005	0.0590	-0.1124
60X	-0.4135	-0.4033	-0.4085	-0.4065	-0.4094	2.0412
1Y	-0.6674	0.8302	-0.6161	1.6604	-0.6000	-0.6071
10Y	-0.6707	-0.5971	1.8049	-0.5414	0.5690	-0.5647
11Y	-0.5134	-0.4205	-0.3242	2.0350	-0.4643	-0.3125
60Y	-1.8303	0.3463	0.3091	-0.3850	0.5936	0.9664
1Z	-0.6464	0.9058	-0.6289	1.6110	-0.6319	-0.6096
10Z	-0.6511	-0.5644	1.8629	-0.5637	0.4408	-0.5245
11Z	-0.4841	-0.3969	-0.4087	2.0394	-0.3932	-0.3565
60Z	-1.8696	0.8107	0.0317	-0.1875	0.7987	0.4160

improve classification performance, the fuzzy matrix has to be standardized as:

$$r_{ik}^{'} = \frac{r_{ik} - \bar{r}_k}{S_k},\ i = 1, 2 \ldots n,\ \ k = 1, 2 \ldots m \tag{4}$$

where,

$$\bar{r}_k = \frac{1}{n}\sum_{i=1}^{n} r_{ik}, S_k = \left[\frac{1}{n-1}\sum_{i=1}^{n}(r_{ik} - \bar{r}_k)^2\right]^{\frac{1}{2}} \tag{5}$$

Fault data classification used in fuzzy mathematics is hierarchical clustering method, and it can be described by three main steps,

(1) Each known sample data is assumed to belong to one type of fault. The distance between any two sample data is calculated, and two samples which have shortest distance will be combined into a new class (new type of fault).
(2) Repeat step one until all samples are combined to one class.
(3) Select the threshold and decide the number of fault type.

Figure 9 shows that the motor can be classified as five types of faults if the value of selected threshold T is larger than any of V1–V5 but less than any of V6–V8. S1–S9 presents samples of faulty PMSM.

2.3.2 *Applying fuzzy mathematics for motor fault classification*

The motor fault transformation matrix will be built using collected experimental data of no fault condition (NF), MU, SE, DE, IE, and AE conditions. The fault vector can thus be built as:

$$U = \left[NF\ \ MU\ \ SE\ \ DE\ \ IE\ \ AE\right] \tag{6}$$

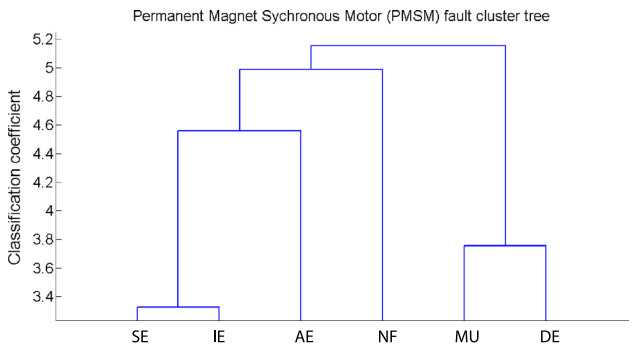

Fig. 11 Clustering tree structure generated by different known types of motor faults

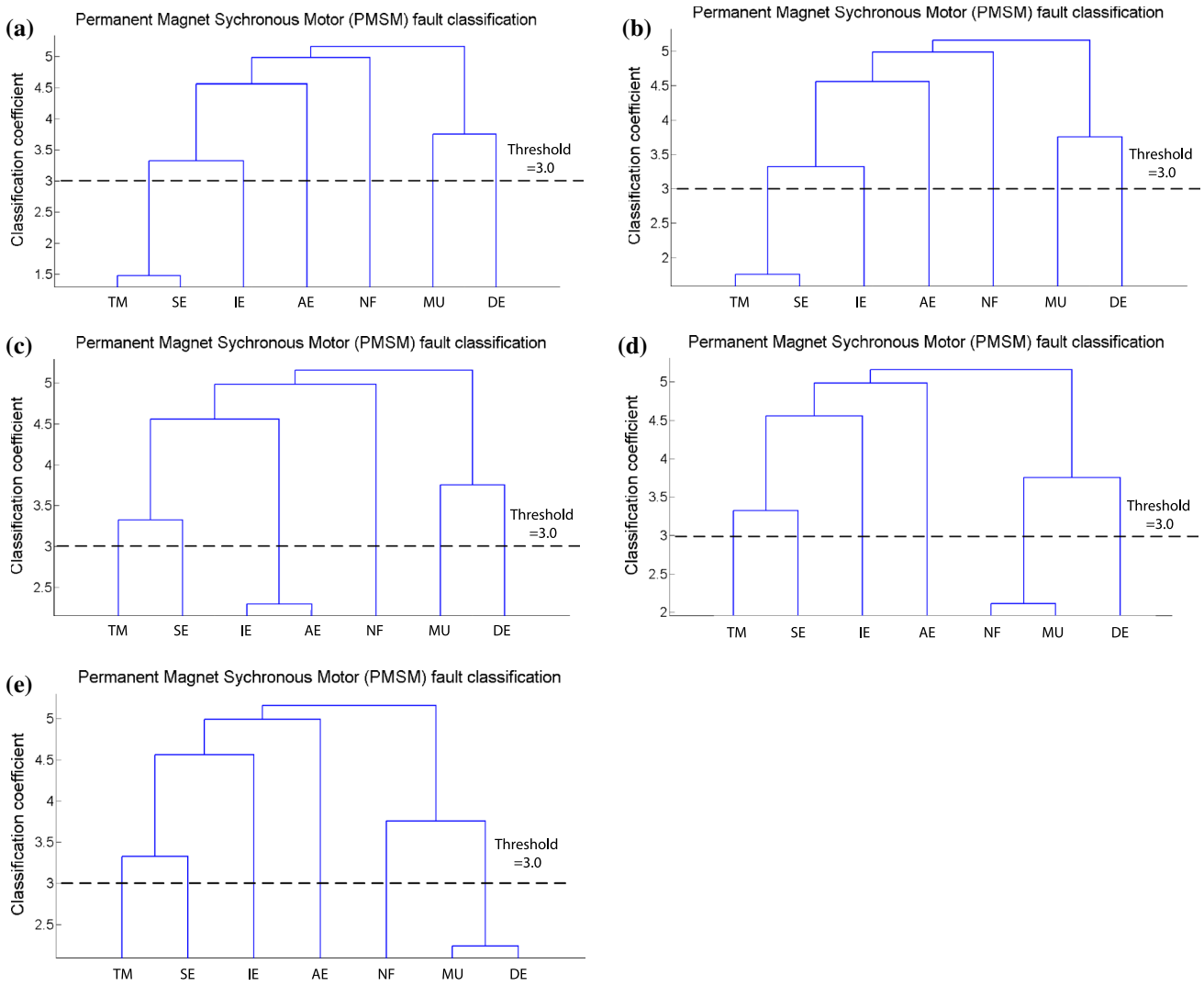

Fig. 12 Cluster tree structure with different types of motor faults: **a** testing motor has a SE fault. **b** Testing motor has an IE fault. **c** Testing motor has an AE fault. **d** Testing motor has a MU fault. **e** Testing motor has a DE fault

The motor fault feature vector can be built based on the signals pattern in Table 2 and expressed as,

$$V = \left[\, 1X \;\; 10X \;\; 11X \;\; 60X \;\; 1Y \;\; 10Y \;\; \ldots\ldots \;\; 1Z \;\; \ldots\ldots \,\right]^T \quad (7)$$

Base on the fault features and fault types shown in Table 2, a standardized fuzzy matrix is built by applying Eq. (4), as shown in Fig. 10.

3 Results and discussion

The largest eccentricity fault (e4) data under different types of eccentricities were selected to develop the fuzzy clustering tree and the result is shown in Fig. 11. Other three eccentricity fault grades were then used to verify the classification algorithm and the classification results with different types of motor faults are shown in Fig. 12. TM in Fig. 12 presents the testing motor which fault is unknown.

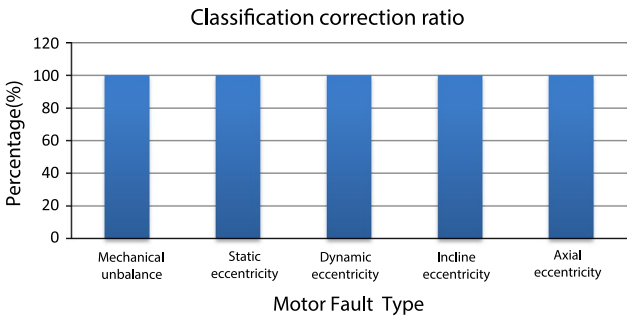

Fig. 13 Classification results by fuzzy cluster tree

Figure 12 shows the cluster tree structure with a motor under monitoring, has the mass eccentricity and four types of UMPs-related faults of M1, respectively. The classification correction ratio is 100 % as shown in Fig. 13.

4 Conclusions

In this paper, a motor with designed mechanical eccentricity (ME), SE, DE, IE, and AE faults were respectively analyzed and tested at no load condition. Fuzzy mathematics classification was employed to do fault classification. The 1×, 10×, 11×, and 60× order of vibration signals in $\boldsymbol{x}$, $\boldsymbol{y}$, and $\boldsymbol{z}$ directions were selected as the fault feature variables, ME, SE, DE, IE, and AE fault were selected as the fault type variables, and all original vibration data were used to form the standardized fuzzy matrix. The experimental results showed that the classification correction ratio is 100 % for MU, SE, DE, IE, and AE fault, respectively. The results proved the effectiveness of the classification algorithm and the future fault detection could thus be faster and more accurate. The limitation of fuzzy mathematic classification is that the fault grade cannot be identified precisely. This problem may be solved by employing genetic programming (GP) in future.

Acknowledgments The authors wish to thank other members in our motor group for their help to do the experimental setup.

References

Bi C, Hla PN, Yu Y, Soh CS, Jiang Q (2011) Influence of axial asymmetrical rotor in PMAC motor operation, ICEMS 2011, Taiwan

Bi C, Liu ZJ, Low TS (1997) Effects of unbalanced magnetic pull in spindle motors. IEEE Trans Magn 33(5):4080–4082

Bi C, Aung NLH, Jiang Q, Lin S (2006) Influence of rotor eccentricity to unbalanced-magnetic-pull in pm synchronous motor, ICEMS06, November 20–23, 2006, Nagasaki, Japan

Concari C, Tassoni C, Toscani A (2010) A new method to discern mechanical unbalances from rotor faults in induction machines, XIX International Conference on Electrical Machines—ICEM 2010, Rome

Guo D, Chu F, Chen D (2002) The unbalanced magnetic pull and its effects on vibration in a three-phase generator with eccentric rotor. J Sound Vib 254(2):297–312

Huang DG (2007) Characteristics of torsional vibrations of a shaft with unbalance. J Sound Vib 308:692–698

Jalan AK, Mohanty AR (2009) Model based fault diagnosis of a rotor–bearing system for misalignment and unbalance under steady-state condition. J Sound Vib 327:604–622

Kim H (2009) On-line mechanical unbalance estimation for permanent magnet synchronous machine drives. IET Electr Power Appl 3(3):178–186

Krysinski T, Malburt F (2007) "Mechanical vibrations active and passive control", ISTE, UK254(2)

Ninth International Conference on vibrations in rotating machinery (2008) vol 2, University of Exeter, UK 8–10 Sept 2008

Sudhakar GNDS, Sekhar AS (2011) Identification of unbalance in a rotor bearing system. J Sound Vib 330:2299–2313

Yu Y, Bi C, Hla PN, Jiang Q, Lin S, Aung NLH, Mamun AL (2012) 3D influence of unbalanced magnetic pull induced by misalignment rotor in PMSM, APMRC2012, Oct 31–Nov 2, 2012, Singapore